

# ANALYSIS OF NONLINEAR DEVIATION IN A GENERALIZED LONGITUDINAL STRONG FOCUSING UNIT

Z. Li, Z. Pan, J. Tang, C. X. Tang\*

Department of Engineering Physics, Tsinghua University, Beijing, China

X. J. Deng, A. Chao<sup>1</sup>

Institute for Advanced Study, Tsinghua University, Beijing, China

<sup>1</sup>also at Stanford University, Stanford, USA

## Abstract

In a generalized longitudinal strong focusing (GLSF) approach employed in steady-state microbunching (SSMB) storage rings, the objective is to achieve complete cancellation of modulations by ensuring that a particle's longitudinal position remains unchanged after passing through both modulators. This requires effective control over the deviation in longitudinal position, which arises from lattice nonlinearities. This paper derives analytical formulations for the mean and standard deviation of the particle position deviation, expressed in terms of the beam and lattice-dependent parameters. The aim is to provide valuable insights into the system's behavior and enable optimization of the GLSF unit's performance.

## INTRODUCTION

Steady-state microbunching (SSMB) [1–4] storage rings have emerged as a promising candidate solution for high-average-power extreme-ultraviolet (EUV) light sources. In principle, SSMB rings are capable of producing nanometer-long bunches on a turn-by-turn basis, which is a desirable feature for coherent EUV radiation generation. The ability of SSMB to generate ultrashort bunches is enabled by the use of laser modulators with modulation wavelengths significantly shorter than RF cavities employed in conventional storage ring systems.

The generalized longitudinal strong focusing (GLSF) approach [5, 6] has been proposed as an insertion unit within the SSMB storage ring, with the aim of further reducing the achievable bunch length at the radiator location. The mechanism is to leverage the ultra-low vertical eigen-emittance inherent to SSMB storage rings, and project it, rather than the longitudinal eigen-emittance, onto the bunch length at the radiation spot through deliberate vertical-longitudinal coupling.

In a typical layout of a GLSF unit, there are four vertically dispersive lattice segments, denoted as parts 1-4 accordingly, with two laser modulators, MOD1 and MOD2, as demonstrated in Fig. 1. Bunch compression is achieved through the coupling manipulation of part 1, MOD1, and part 2. Given that the SSMB mechanism operates on a turn-by-turn eigen-state basis, the beam status must be recovered to an uncoupled and unmodulated state after radiation and prior to being returned to the storage ring. Accordingly, part 3

is introduced to form, together with part 2, an isochronous achromat that is transparent in the longitudinal dimension, such that MOD2 can directly cancel the impact imposed on the beam by MOD1 through opposite modulation. And finally, part 4 addresses any residual vertical-longitudinal coupling effects.

The modulation cancellation process functions effectively within the realm of linear beam dynamics. However, when accounting for the nonlinear effects arising from the lattice between the laser modulators, the prospect of perfect cancellation can be compromised by the deviation in longitudinal particle positions. This deviation can lead to residual energy spread, which may then degrade the beam dynamics. To address this issue, a straightforward approach is to perform particle tracking and quantify the deviation through statistical analysis. However, this can be time-consuming and require substantial computational resources, as the particle count may be considerable to achieve the desired precision in the statistical results.

The paper proposes an analytical approach to obtain the longitudinal deviation arising from nonlinear effects. It first establishes the connection between the deviation and the particle coordinates at the entry of the lattice of interest via the second-order Taylor-map coefficients. Then, by calculating the second- and fourth-order beam moments at the lattice entrance, the mean and standard deviation of the longitudinal deviation can be derived. These turn out to be functions of beam parameters, such as emittances and natural energy spread, as well as lattice-dependent parameters, including the Taylor-map coefficients and Courant-Snyder functions. This analytical methodology can avoid the need for extensive particle tracking, while directly providing the result. Furthermore, the analytical expression of the longitudinal deviation induced by lattice nonlinearity delivers valuable insights into beam dynamics of the system. We believe this approach can also be applied to various research concerning lattice nonlinear effects.

## METHODOLOGY

The nonlinear behavior of a lattice segment can be characterized by the Taylor-map representation, which takes the following mathematical form:

$$\Delta u_{i\_out} = \sum_{j,k} T_{ijk} u_{j\_in} u_{k\_in} \quad (i, j, k = 1, \dots, 6) \quad (1)$$

\* tang.xuh@tsinghua.edu.cn

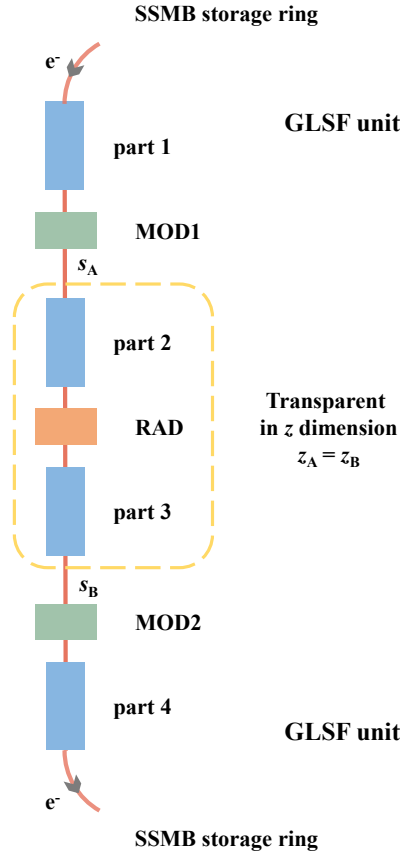


Figure 1: GLSF unit layout and modulation cancellation components (yellow dashed box)

In this representation,  $u_1$  through  $u_6$  denote the particle coordinates  $(x, x', y, y', z, \delta)$ , respectively. The subscripts  $_{in}$  and  $_{out}$  denote the entry and exit of the lattice segment of interest.  $T_{ijk}$  are the Taylor-map coefficients, which specify the contribution of the product of coordinates  $u_j$  and  $u_k$  at the lattice entry to the coordinate  $u_i$  at the lattice exit.

Returning to the issue of GLSF modulation cancellation, the lattice segment of interest is situated between MOD1 and MOD2, as marked by the yellow dashed box in Fig. 1. Its entry is denoted as  $s_A$ . The key particle coordinate at the exit of this lattice segment is the nonlinear deviation  $\Delta z$ , whose statistical properties, specifically the mean  $\langle \Delta z \rangle$  and standard deviation  $\sigma_{\Delta z}$ , are of importance.

The workflow of this analytical method can then be summarized as follows:

- Express  $\Delta z$  in terms of the particle coordinates at  $s_A$  using the Taylor-map representation.
- Derive the expressions for  $\langle \Delta z \rangle$  and  $\sigma_{\Delta z}$ .
- Evaluate the 2nd and 4th-order beam moments at  $s_A$  and substitute them into  $\langle \Delta z \rangle$  and  $\sigma_{\Delta z}$  expressions.
- Sort expressions for  $\langle \Delta z \rangle$  and  $\sigma_{\Delta z}$  by beam parameters, namely  $\epsilon_x, \epsilon_y, \sigma_{\delta_0}$ , as well as  $h$ .

Here,  $\epsilon_x$  and  $\epsilon_y$  denote the horizontal and vertical eigen-emittances, while  $\sigma_{\delta_0}$  represents the natural energy spread. And  $h$  is the modulation strength of MOD1. The first three steps of the workflow are covered here, while the results of the final step are demonstrated in the following section.

For a lattice segment with vertically bending magnets, the nonlinear deviation  $\Delta z$  can be expressed as:

$$\Delta z = T_{511}x_A^2 + 2T_{521}x_Ax'_A + T_{522}x'^2_A + T_{533}y_A^2 + 2T_{543}y_Ay'_A + T_{544}y'^2_A + 2T_{563}y_A\delta_A + 2T_{564}y'_A\delta_A + T_{566}\delta_A^2 \quad (2)$$

Then for  $\langle \Delta z \rangle$  and  $\sigma_{\Delta z} = \sqrt{\langle (\Delta z)^2 \rangle - \langle \Delta z \rangle^2}$ , there are:

$$\begin{aligned} \langle \Delta z \rangle &= T_{511}\langle x_A^2 \rangle + 2T_{521}\langle x_Ax'_A \rangle + T_{522}\langle x'^2_A \rangle \\ &+ T_{533}\langle y_A^2 \rangle + 2T_{543}\langle y_Ay'_A \rangle + T_{544}\langle y'^2_A \rangle \\ &+ 2T_{563}\langle y_A\delta_A \rangle + 2T_{564}\langle y'_A\delta_A \rangle + T_{566}\langle \delta_A^2 \rangle \end{aligned} \quad (3)$$

$$\begin{aligned} \sigma_{\Delta z}^2 &= T_{511}^2(\langle x^4 \rangle - \langle x^2 \rangle^2) + 4T_{511}T_{521}(\langle x^3x' \rangle - \langle x^2 \rangle \langle xx' \rangle) \\ &+ 2T_{511}T_{522}(\langle x^2x'^2 \rangle - \langle x^2 \rangle \langle x'^2 \rangle) + 4T_{521}^2(\langle x^2x'^2 \rangle - \langle xx' \rangle^2) \\ &+ T_{522}^2(\langle x'^4 \rangle - \langle x'^2 \rangle^2) + 4T_{521}T_{522}(\langle xx'^3 \rangle - \langle xx' \rangle \langle x'^2 \rangle) \\ &+ 2T_{511}T_{533}(\langle x^2y^2 \rangle - \langle x^2 \rangle \langle y^2 \rangle) + 2T_{511}T_{544}(\langle x^2y'^2 \rangle - \langle x^2 \rangle \langle y'^2 \rangle) \\ &+ 4T_{511}T_{543}(\langle x^2yy' \rangle - \langle x^2 \rangle \langle yy' \rangle) + 2T_{511}T_{566}(\langle x^2\delta^2 \rangle - \langle x^2 \rangle \langle \delta^2 \rangle) \\ &+ 4T_{511}T_{563}(\langle x^2y\delta \rangle - \langle x^2 \rangle \langle y\delta \rangle) + 4T_{511}T_{564}(\langle x^2y'\delta \rangle - \langle x^2 \rangle \langle y'\delta \rangle) \\ &+ 4T_{521}T_{533}(\langle xx'y^2 \rangle - \langle xx' \rangle \langle y^2 \rangle) + 4T_{521}T_{544}(\langle xx'y'^2 \rangle - \langle xx' \rangle \langle y'^2 \rangle) \\ &+ 8T_{521}T_{543}(\langle xx'yy' \rangle - \langle xx' \rangle \langle yy' \rangle) + 4T_{521}T_{566}(\langle xx'\delta^2 \rangle - \langle xx' \rangle \langle \delta^2 \rangle) \\ &+ 8T_{521}T_{563}(\langle xx'y\delta \rangle - \langle xx' \rangle \langle y\delta \rangle) + 8T_{521}T_{564}(\langle xx'y'\delta \rangle - \langle xx' \rangle \langle y'\delta \rangle) \\ &+ 2T_{522}T_{533}(\langle x'^2y^2 \rangle - \langle x'^2 \rangle \langle y^2 \rangle) + 2T_{522}T_{544}(\langle x'^2y'^2 \rangle - \langle x'^2 \rangle \langle y'^2 \rangle) \\ &+ 4T_{522}T_{543}(\langle x'^2yy' \rangle - \langle x'^2 \rangle \langle yy' \rangle) + 2T_{522}T_{566}(\langle x'^2\delta^2 \rangle - \langle x'^2 \rangle \langle \delta^2 \rangle) \\ &+ 4T_{522}T_{563}(\langle x'^2y\delta \rangle - \langle x'^2 \rangle \langle y\delta \rangle) + 4T_{522}T_{564}(\langle x'^2y'\delta \rangle - \langle x'^2 \rangle \langle y'\delta \rangle) \\ &+ T_{533}^2(\langle y^4 \rangle - \langle y^2 \rangle^2) + 4T_{533}T_{543}(\langle y^3y' \rangle - \langle y^2 \rangle \langle yy' \rangle) \\ &+ 4T_{543}^2(\langle y^2y'^2 \rangle - \langle yy' \rangle^2) + 2T_{533}T_{544}(\langle y^2y'^2 \rangle - \langle y^2 \rangle \langle y'^2 \rangle) \\ &+ T_{544}^2(\langle y'^4 \rangle - \langle y'^2 \rangle^2) + 4T_{543}T_{544}(\langle yy'^3 \rangle - \langle yy' \rangle \langle y'^2 \rangle) \\ &+ 4T_{533}T_{563}(\langle y^3\delta \rangle - \langle y^2 \rangle \langle y\delta \rangle) + 4T_{533}T_{564}(\langle y^2y'\delta \rangle - \langle y^2 \rangle \langle y'\delta \rangle) \\ &+ 8T_{543}T_{563}(\langle y^2y'\delta \rangle - \langle yy' \rangle \langle y\delta \rangle) + 8T_{543}T_{564}(\langle yy'^2\delta \rangle - \langle yy' \rangle \langle y'\delta \rangle) \\ &+ 4T_{544}T_{563}(\langle yy'^2\delta \rangle - \langle y'^2 \rangle \langle y\delta \rangle) + 4T_{544}T_{564}(\langle y'^3\delta \rangle - \langle y'^2 \rangle \langle y'\delta \rangle) \\ &+ 2T_{533}T_{566}(\langle y^2\delta^2 \rangle - \langle y^2 \rangle \langle \delta^2 \rangle) + 2T_{544}T_{566}(\langle y'^2\delta^2 \rangle - \langle y'^2 \rangle \langle \delta^2 \rangle) \\ &+ 4T_{543}T_{566}(\langle yy'\delta^2 \rangle - \langle yy' \rangle \langle \delta^2 \rangle) + 8T_{563}T_{564}(\langle yy'\delta^2 \rangle - \langle y\delta \rangle \langle y'\delta \rangle) \\ &+ 4T_{563}^2(\langle y^2\delta^2 \rangle - \langle y\delta \rangle^2) + 4T_{563}T_{566}(\langle y\delta^3 \rangle - \langle y\delta \rangle \langle \delta^2 \rangle) \\ &+ 4T_{564}^2(\langle y'^2\delta^2 \rangle - \langle y'\delta \rangle^2) + 4T_{564}T_{566}(\langle y'\delta^3 \rangle - \langle y'\delta \rangle \langle \delta^2 \rangle) \\ &+ T_{566}^2(\langle \delta^4 \rangle - \langle \delta^2 \rangle^2). \end{aligned} \quad (4)$$

Note that for the sake of conciseness, the subscript of  $_A$  has been omitted for  $(x, x', y, y', \delta)$  in the expression above.

The second-order beam moments at  $s_A$  are given by:

$$\begin{aligned} \langle x_A^2 \rangle &= \epsilon_x \beta_{xA} \quad \langle x_Ax'_A \rangle = -\epsilon_x \alpha_{xA} \quad \langle x'^2_A \rangle = \epsilon_x \gamma_{xA} \\ \langle y_A^2 \rangle &= \epsilon_y \beta_{yA} + D_A^2 \sigma_{\delta_0}^2 \quad \langle y_A\delta_A \rangle = D_A \sigma_{\delta_0}^2 \\ \langle y'^2_A \rangle &= \epsilon_y \gamma_{yA} + D_A'^2 \sigma_{\delta_0}^2 \quad \langle y'_A\delta_A \rangle = D_A' \sigma_{\delta_0}^2 \\ \langle y_Ay'_A \rangle &= -\epsilon_y \alpha_{yA} + D_A D_A' \sigma_{\delta_0}^2 \quad \langle \delta_A^2 \rangle = \sigma_{\delta_0}^2 + \frac{h^2}{2k^2} \end{aligned} \quad (5)$$

Here,  $(\alpha, \beta, \gamma)$  and  $(D, D')$  are the Courant-Snyder and vertical dispersion functions, and  $k$  is the modulation wave number of MOD1.

Additionally, the beam is uncoupled between the  $(x, x')$  and  $(y, y', \delta)$  dimensions at  $s_A$ . Consequently, the following beam moments vanish:

$$\begin{aligned} \langle x_A y_A \rangle &= 0 & \langle x_A y'_A \rangle &= 0 & \langle x_A \delta_A \rangle &= 0 \\ \langle x'_A y_A \rangle &= 0 & \langle x'_A y'_A \rangle &= 0 & \langle x'_A \delta_A \rangle &= 0 \end{aligned} \quad (6)$$

The fourth-order beam moments can be derived from the second-order moments using the following relationship:

$$\langle X_i X_j X_k X_n \rangle = \langle X_i X_j \rangle \langle X_k X_n \rangle + \langle X_i X_k \rangle \langle X_j X_n \rangle + \langle X_i X_n \rangle \langle X_j X_k \rangle \quad (7)$$

It should be noted that this law applies for multivariate Gaussian distributions  $X$ . Appropriate adjustments must be made when handling the non-Gaussian distribution of  $\delta_A$  due to the sinusoidal modulation introduced by MOD1.

## RESULTS

The expressions for the mean  $\langle \Delta z \rangle$  and standard deviation  $\sigma_{\Delta z}$  of the nonlinear deviation  $\Delta z$  are then sorted by beam parameters, namely  $\epsilon_x$ ,  $\epsilon_y$ ,  $\sigma_{\delta_0}$ , and  $h$ , as shown below:

$$\begin{aligned} \langle \Delta z \rangle &= \epsilon_x \Omega_1 + \epsilon_y \Omega_2 + \sigma_{\delta_0}^2 \Omega_3 + \frac{h^2}{2k^2} \Omega_4 \\ \sigma_{\Delta z}^2 &= \epsilon_x^2 \Sigma_1 + \epsilon_y^2 \Sigma_2 + \epsilon_y \sigma_{\delta_0}^2 \Sigma_3 + \epsilon_y \frac{h^2}{k^2} \Sigma_4 \\ &+ \sigma_{\delta_0}^4 \Sigma_5 + \sigma_{\delta_0}^2 \frac{h^2}{k^2} \Sigma_6 + \frac{h^4}{k^4} \Sigma_7 \end{aligned} \quad (8)$$

The corresponding coefficients  $\Omega_1 - \Omega_4$  and  $\Sigma_1 - \Sigma_7$  are all composed of lattice-dependent parameters and are given as follows:

$$\begin{aligned} \Omega_1 &= T_{511} \beta_x - 2T_{521} \alpha_x + T_{522} \gamma_x \\ \Omega_2 &= T_{533} \beta_y - 2T_{543} \alpha_y + T_{544} \gamma_y \\ \Omega_3 &= T_{533} D^2 + 2T_{543} D D' + T_{544} D'^2 + 2T_{563} D + 2T_{564} D' \\ &+ T_{566} \\ \Omega_4 &= T_{566} \\ \Sigma_1 &= 2\Omega_1^2 + 4(T_{521}^2 - T_{511} T_{522}) \\ \Sigma_2 &= 2\Omega_2^2 + 4(T_{543}^2 - T_{533} T_{544}) \\ \Sigma_3 &= 4\Omega_2 (\Omega_3 - T_{566}) \\ &+ 4(T_{543}^2 - T_{533} T_{544}) (\gamma_y D^2 + 2\alpha_y D D' + \beta_y D'^2) \\ &+ 4(T_{563}^2 \beta_y - 2T_{563} T_{564} \alpha_y + T_{564}^2 \gamma_y) T_{566} \\ &+ 8(T_{543} T_{564} - T_{544} T_{563}) (\gamma_y D + \alpha_y D') \\ &+ 8(T_{543} T_{563} - T_{533} T_{564}) (\beta_y D' + \alpha_y D) \\ \Sigma_4 &= 2(T_{563}^2 \beta_y - 2T_{563} T_{564} \alpha_y + T_{564}^2 \gamma_y) \\ \Sigma_5 &= 2\Omega_3^2 \\ \Sigma_6 &= 2(T_{563} D + T_{564} D' + T_{566})^2 \\ \Sigma_7 &= \frac{1}{8} T_{566}^2 \end{aligned} \quad (9)$$

For conciseness, the subscript  $A$  has been omitted in the expressions above for  $(\alpha_x, \beta_x, \gamma_x, \alpha_y, \beta_y, \gamma_y, D, D')$ .

## DISCUSSION

The expressions given in Eq. (8) provide valuable insights into the contribution of various beam parameters to the nonlinear deviation  $\Delta z$ , and further outline the criteria for controlling the corresponding coefficients. For instance, the beam parameters are assumed to be  $(\epsilon_x, \epsilon_y, \sigma_{\delta_0}, |h|, k) = (1 \text{ nm-rad}, 1 \text{ pm-rad}, 2.5 \times 10^{-4}, 4000 \text{ m}^{-1}, 6.28 \times 10^6 \text{ m}^{-1})$ . If the nonlinear deviation  $\sigma_{\Delta z}$  is to be controlled below 1 nm, the corresponding coefficients should be limited by at least the following constraints:  $(\Sigma_1, \Sigma_2, \Sigma_3, \Sigma_4, \Sigma_5, \Sigma_6, \Sigma_7) < (1, 1 \times 10^6, 16 \text{ m}, 2 \text{ m}, 2 \times 10^{-4} \text{ m}^2, 4 \times 10^{-5} \text{ m}^2, 6 \times 10^{-6} \text{ m}^2)$ . These conclusions are expected to prove valuable in future lattice optimization.

In practice, the  $\Sigma$  coefficients of  $\sigma_{\Delta z}$  are perhaps of greater focus than the  $\Omega$  coefficients of  $\langle \Delta z \rangle$ , as controlling  $\sigma_{\Delta z}$  is more likely to result in a controlled  $\langle \Delta z \rangle$ , whereas the opposite is not necessarily the case. Additionally, the effects of  $\langle \Delta z \rangle$  can be somewhat compensated by introducing a phase shift in the MOD2 modulation. A  $\sigma_{\Delta z}$  of 0.1 nm has been realized in recent work under the following conditions:  $\epsilon_x = 5.1 \text{ nm-rad}$ ,  $\epsilon_y = 4.6 \text{ pm-rad}$ ,  $\sigma_{\delta_0} = 9.4 \times 10^{-4}$ ,  $h = 2560 \text{ m}^{-1}$ , and  $k = 1.2 \times 10^7 \text{ m}^{-1}$ . And the corresponding  $\langle \Delta z \rangle$  is 0.05 nm.

Furthermore, the analytical approach detailed in this work is anticipated to find broader application in research exploring the nonlinear effects within lattice segments, such as the evaluation of distortions to the beam distribution in the transverse phase space.

## CONCLUSION

In this paper, we present an analytical approach for evaluating the nonlinear deviation of the longitudinal position  $\Delta z$  within the lattice segment situated between modulators in the GLSF unit. By adopting the Taylor-map representation of lattice nonlinearity and the beam moments at the lattice entrance, the statistical properties of  $\Delta z$ , sorted by beam parameters, are provided. This analytical approach can eliminate the need for extensive particle tracking simulations and is foreseen to have wide applicability across nonlinear investigations. The derived expressions for the mean  $\langle \Delta z \rangle$  and, in particular, standard deviation  $\sigma_{\Delta z}$  of  $\Delta z$  are believed to be capable of providing useful insights for future lattice design and optimization efforts.

## ACKNOWLEDGEMENTS

This work is supported by National Key R&D Program of China (Grant No. 2022YFA1603400), National Natural Science Foundation of China (NSFC Grant No. 12035010), and Tsinghua University Initiative Scientific Research Program.

## REFERENCES

- [1] D. Ratner and A. Chao, "Steady-state microbunching in a storage ring for generating coherent radiation", *Phys. Rev. Lett.*, vol. 105, no. 15, p. 154801, 2010. doi:10.1103/PhysRevLett.105.154801

- [2] A. Chao *et al.*, "High Power Radiation Sources using the Steady-state Microbunching Mechanism", in *Proc. IPAC'16*, Busan, Korea, June 2016, pp. 1048-1053. doi:10.18429/JACoW-IPAC2016-TUXB01 pp. 576–579, 2021. doi:10.1038/s41586-021-03203-0
- [3] C. Tang *et al.*, "An Overview of the Progress on SSMB", in *Proc. FLS'18*, Shanghai, China, June 2018, pp. 166-170. doi: 10.18429/JACoW-FLS2018-THP2WB02
- [4] X. Deng *et al.*, "Experimental demonstration of the mechanism of steady-state microbunching", *Nature*, vol. 590, no. 7847, pp. 576–579, 2021. doi:10.1038/s41586-021-03203-0
- [5] Z. Li *et al.*, "Generalized longitudinal strong focusing in a steady-state microbunching storage ring", *Phys. Rev. Accel. Beams*, vol. 26, no. 11, p. 110701, 2023. doi:10.1103/PhysRevAccelBeams.26.110701
- [6] Z. Li *et al.*, "Generalized longitudinal strong focusing in a storage ring for coherent EUV radiation", in *Proc. IPAC'23*, Venice, Italy, May 2023, pp. 1134-1136. doi:10.18429/JACoW-IPAC2023-MOPM065